

III.4.5 Electron-positron circular colliders

Frank Zimmermann

CERN, Geneva, Switzerland

In the late 1950s and early 1960s an Italian group at the Laboratori Nazionali di Frascati, led by Bruno Touschek, designed, built and operated the first electron-positron collider AdA, with a luminosity of order $10^{25} \text{ cm}^{-2}\text{s}^{-1}$ [1]. AdA was followed by an impressive sequence of colliders of ever increasing energy, luminosity, and size. The luminosity of e^+e^- colliders increased by more than ten orders of magnitude, without any indication of saturation yet, as is illustrated in Fig. III.4.1, which also includes an extrapolation to the coming decades.

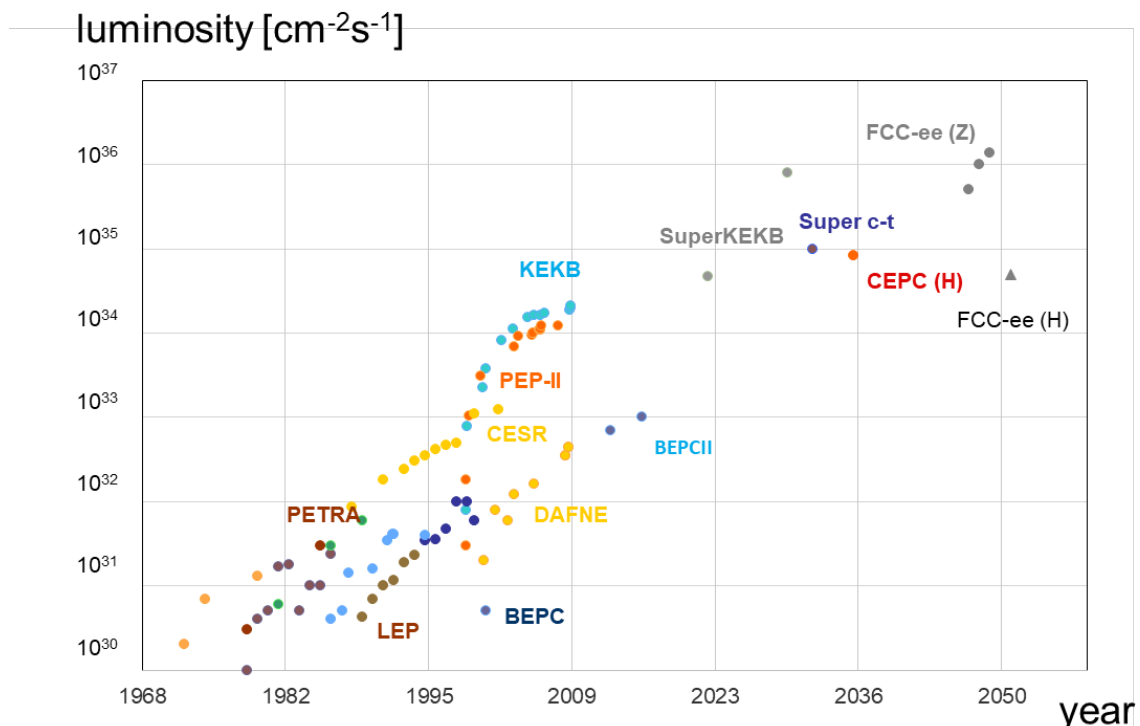


Fig. III.4.1: Luminosity of past, present and future circular e^+e^- colliders versus year. Until 2023 achieved luminosities are presented. Beyond the year 2023, luminosity forecasts for SuperKEKB and for the two proposed Super charm-tau factories [2,3], CEPC, and FCC-ee are indicated (Courtesy Y. Funakoshi, 2016; updated).

In total, 22 circular e^+e^- colliders have so far reached the operational stage (some in several successive configurations) and five of these are operational now (2023), namely DAΦNE in Italy, SuperKEKB in Japan, BEPCII in China, and VEPP2000 plus VEPP-4M in Russia [4]—see Table III.4.1. Asymmetric energies of the two beams, such as used at KEKB, PEP-II and SuperKEKB, allow for enhanced flavour-physics research and for interesting interaction-region designs.

Considering the near head-on collision of two particles of masses m_1 and m_2 with energies E_1

This section should be cited as: Electron-positron circular colliders, F. Zimmermann, DOI: [10.23730/CYRSP-2024-003.1981](https://doi.org/10.23730/CYRSP-2024-003.1981), in: Proceedings of the Joint Universities Accelerator School (JUAS): Courses and exercises, E. Métral (ed.), CERN Yellow Reports: School Proceedings, CERN-2024-003, DOI: [10.23730/CYRSP-2024-003](https://doi.org/10.23730/CYRSP-2024-003), p. 1981. © CERN, 2024. Published by CERN under the [Creative Commons Attribution 4.0 license](https://creativecommons.org/licenses/by/4.0/).

Table III.4.1: Selected past and present circular electron-positron colliders: their maximum beam energy E_b , ring circumference C , peak luminosity \mathcal{L}_{\max} , and years of luminosity operation; † achieved; * design; the luminosity is defined in Eq. (III.4.4) and discussed below; from Ref. [4].

collider	E_b [GeV]	C [m]	\mathcal{L}_{\max} [cm ⁻² s ⁻¹]	years of operation
AdA	0.25	4.1	10^{25}	1964
ADONE	1.5	105	6×10^{29}	1969–93
SPEAR	4.2	234	1.2×10^{31}	1972–90
PETRA	23.4	2304	2.4×10^{31}	1978–86
CESR	6	768	1.3×10^{33}	1979–2008
TRISTAN	32	3018	4×10^{31}	1987–95
LEP	104.6	26659	10^{32}	1989–2000
PEP-II	3.1+9	2200	1.2×10^{34}	1999–2008
KEKB	3.5+8.0	3016	2.1×10^{34}	1999–2010
VEPP-4M	6	366	2×10^{31}	1979–
BEPC/II	2.3	238	10^{33}	1989–
DAΦNE	0.51	98	4.5×10^{32}	1997–
VEPP2000	1.0	24	4×10^{31}	2010–
SuperKEKB	7+4	3016	4.7×10^{34} † 8×10^{35} *	2018–

and E_2 colliding at a crossing angle θ_c , the centre-of-mass energy (c.m., or cm) E_{cm} is

$$E_{\text{cm}} = \left(2E_1E_2 + (m_1^2 + m_2^2)c^4 + 2 \cos \theta_c \sqrt{E_1^2 - m_1^2c^4} \sqrt{E_2^2 - m_2^2c^4} \right)^{1/2}, \quad (\text{III.4.1})$$

where c denotes the speed of light. Figure III.4.2 presents the peak luminosity of different past colliders, and several proposed future colliders as a function of centre-of-mass energy.

Two important limitations of circular colliders are synchrotron radiation and beam-beam effects, which we will discuss next.

III.4.5.1 Synchrotron radiation

Electron or positron beams circulating in a storage ring emit synchrotron radiation. The average energy loss per turn depends on the bending radius ρ and increases with the fourth power of beam energy E_b , $\Delta E_{\text{SR}} = C_\gamma E_b^4 / \rho$, with $C_\gamma \approx 8.85 \times 10^5 \text{ m GeV}^{-3}$ [5]. Considering two countercirculating beams of equal energy and average beam current I_b , the total synchrotron radiation power of a collider is

$$P_{\text{SR}} = 2I_b \cdot \Delta E_{\text{SR}}. \quad (\text{III.4.2})$$

At high beam energy, the beam current I_b is limited by the available electrical power, required by the radiofrequency system to compensate for the radiated energy loss, which typically amounts to 1.5–2 times the synchrotron radiation power, taking into account various system inefficiencies.

III.4.5.2 Beam-beam effects

Another prominent limitation of circular collider performance arises from the electric and magnetic fields of the opposite bunch at the interaction point (IP). The resulting beam-beam forces are characterized by the dimensionless horizontal or vertical beam-beam parameter [6]:

$$\xi_{x,y} = \frac{r_e N_b \beta_{x,y}^*}{2\pi \gamma \sigma_{x,y}^* (\sigma_x^* + \sigma_y^*)} H_\xi(\theta_c, \sigma_z / \beta_y^*), \quad (\text{III.4.3})$$

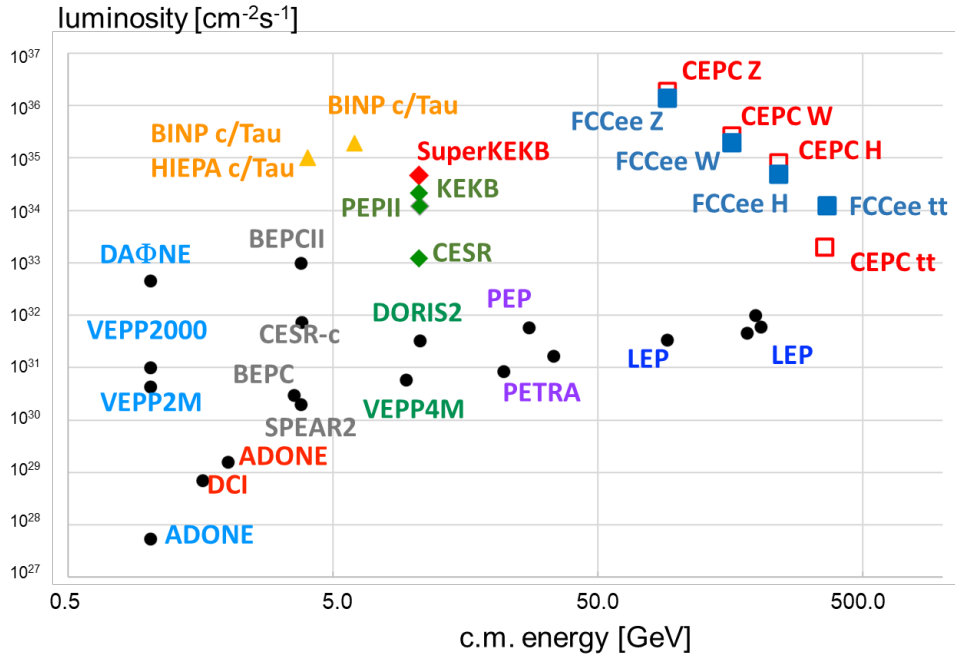


Fig. III.4.2: Luminosity of past, present and future circular e^+e^- colliders versus c.m. energy (Courtesy M. Biagini, 2023).

where $r_e = e^2/(4\pi\epsilon_0 m_e c^2)$ denotes the classical electron radius, e the electron charge, ϵ_0 the permittivity of free space, m_e the electron mass, N_b the bunch population of the opposite beam, $\beta_{x,y}^*$ the horizontal or vertical beta function of the beam experiencing the force, γ its relativistic Lorentz factor, and $\sigma_{x,y}^*$ the horizontal or vertical rms beam size of the opposite beam, respectively. The asterisk indicates values at the IP, and H_ξ is a geometric function, which depends on the crossing angle θ_c and on the so-called “hourglass effect” (variation of the beta function over the length of the collision), that is on the ratio of rms bunch length σ_z of the opposite beam to β_y^* . The beam-beam parameter is roughly equal to the betatron tune shift experienced by small-amplitude particles. It is positive in the case of opposite-charge beams, like e^+e^- .

Beam-beam forces can also lead to coherent effects, such as unstable beam oscillations [7–10] or the blow-up of one beam’s size while the other beam remains small or even shrinks (beam-beam “flip-flop” effect) [11, 12]. Recently, a new coherent instability was discovered, linking longitudinal and transverse motion in collisions with a large crossing angle [13].

In addition, the tune spread arising from ξ and the non-linear nature of the beam-beam interaction may result in strong diffusion along medium- or high-order resonances $kQ_x + lQ_y + mQ_z = n$ (with $Q_{z,x,y}$ denoting the synchrotron and betatron tunes, and k, l, m and n representing integers) and, ultimately, in beam size growth and beam losses. For e^+e^- colliders the empirical beam-beam limit is about an order of magnitude larger than in hadron colliders [14], with maximum $\xi_{x,y} \approx 0.03 - 0.12$ [15].

For a circular electron-positron collider operating at the beam-beam limit (maximum achievable or acceptable value of ξ_y), the luminosity is proportional to the beam current I_b ,

$$\mathcal{L} \approx f_{\text{rev}} \gamma \frac{I_b \xi_y}{2e r_e \beta_y^*} \left(1 + \frac{\sigma_y^*}{\sigma_x^*} \right), \quad (\text{III.4.4})$$

where $f_{\text{rev}} (= c/C)$ denotes the revolution frequency. A geometric luminosity factor H_L , which again depends on the crossing angle and on the hourglass effect, is roughly canceled by the factor H_ξ , so that

both H_L and H_ξ were omitted in the luminosity formula (III.4.4).

From Eq. (III.4.4), we note that higher luminosity can be achieved by increasing the beam current I_b , decreasing the vertical beta function β_y^* , and also by pushing up the beam-beam parameter ξ_y . The maximum achievable beam-beam tune-shift increases at high energy in presence of strong radiation damping [16].

Over the decades several methods have been implemented to overcome, or boost, the beam-beam limit, including: a) carefully choosing working tunes (Q_x, Q_y) away from the most detrimental resonances; b) operation with very flat bunches (wide in the horizontal plane and narrow in the vertical — see Eq. (III.4.3)); c) compensation of the beam-beam effects using electron lenses [17]; d) reduction of the strength of the beam-beam resonance in the *round beam* collision scheme with strongly coupled vertical and horizontal motion [18–21]; e) “crab crossing”, where transversely deflecting cavities are used to convert a collision with crossing angle into an effective head-on collision [22, 23]; and f) by using the so-called “crab-waist” collision method, based on existing or additional sextupole magnets with suitable betatron phase advances to the IP, which modify the vertical focusing as a function of horizontal IP position so as to suppress the excitation of harmful resonances [24–26].

The focusing of the beams during the collision changes the beam optics, especially for low-amplitude particles. Properly choosing the working point in the tune diagram, e.g., just above the half integer resonance in case of e^+e^- collisions with a single IP, leads to a reduction of the effective beta function at the collision point, the “dynamic beta” effect [27]. In circular e^+e^- colliders, this optics change in collision, propagating all around the ring, also modifies the equilibrium horizontal emittance ε_x , which is known as “dynamic emittance” [12, 28]. The net IP beam sizes then follow from the combined change of β^* and ε_x . Parameters are normally chosen so that the overall dynamic effect increases the luminosity.

For the highest energy colliders and with very small collision spot sizes, beamstrahlung, that is the synchrotron radiation emitted during the collision in the field of the opposite beam, gives rise to additional new beam-beam phenomena, a reduction in beam lifetime [29, 30] (also see Eq. (III.4.6) below), an increase in energy spread and bunch length [31], or enhanced beam-beam flip-flop effects [32].

III.4.5.3 SuperKEKB

Since 2018 SuperKEKB operates with 7 GeV electron and 4 GeV positron beams. It is aiming for ultimate luminosities well above $10^{35} \text{ cm}^{-2}\text{s}^{-1}$. In summer 2022, a world record luminosity of $4.7 \times 10^{34} \text{ cm}^{-2}\text{s}^{-1}$ was reached, still at beam currents much lower than the design [33]. The integrated luminosity, and also the integrated weekly luminosity, continuously increased during the first three years of running and despite long down periods between rather short runs; see Fig. III.4.3.

Vertical beam-beam tune shifts of $\xi_y \approx 0.05$ for the 4 GeV positron beam, and $\xi_y \approx 0.03$ for the 7 GeV electron beam were achieved. These values are still about a factor of two lower than those obtained at the previous KEKB collider. So far, SuperKEKB routinely has run with a small vertical interaction-point beta function of $\beta_y^* = 1 \text{ mm}$, and also 0.8 mm has already been demonstrated. Since 2020 SuperKEKB operates with a virtual crab-waist collision scheme, first developed for the FCC-ee design, where the strength of an existing sextupole magnet is reduced to create the crab waist [35]. The original crab-waist scheme, using additional sextupole magnets, was earlier implemented at DAΦNE [25]. In general, the crab-waist concept combines a large Piwinski angle Φ , and an extremely low vertical IP beta function β_y^* ($\ll \sigma_z$) with the aforementioned cancellation of transverse betatron resonances of the form $kQ_x + lQ_y = n$ (k, l, n integer) through sextupole magnets [24]. The crab-waist collision scheme has become a design choice for all proposed future e^+e^- circular colliders.

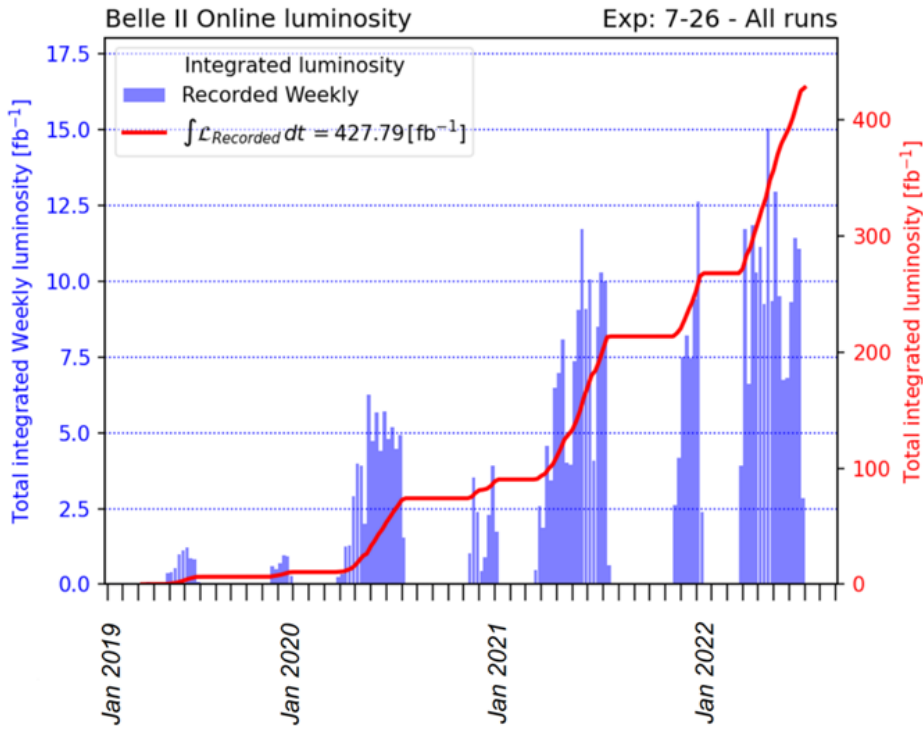


Fig. III.4.3: Total and weekly integrated luminosity of SuperKEKB during the first years of beam commissioning [34]. In the summer of 2022, the beam operation was halted for more than 18 months.

III.4.5.4 Higgs, electroweak and top quark factories

First hints at a Higgs boson with a mass around 125 GeV from the LHC experiments in 2011 motivated a proposal for constructing a circular e^+e^- collider as a high-luminosity Higgs factory [36], and led to a renewed interest in energy-frontier circular e^+e^- colliders. Importantly, the latter could also serve as the first stage of a future hadron collider, by providing the tunnel and large portions of the technical infrastructure, similar to how LEP paved the way for the LHC.

Most of the Higgs factories proposed today aim at improving the precision of coupling measurements of Higgs boson, top quark, W and Z by an order of magnitude or more compared with the state of the art. Two specific proposals for circular e^+e^- colliders with ~ 100 km circumference have gained momentum: the Future Circular electron-positron Collider (FCC-ee) at CERN [37] and the Circular Electron-Positron Collider (CEPC) in China [38]. The FCC-ee collider is sketched in Fig. III.4.4.

The design of these machines limits the total synchrotron radiation $P_{\text{SR}} = 2I_b \cdot \Delta E_{\text{SR}}$ to values of order 100 MW, and it assumes operation at the beam-beam limit ξ_y . These two conditions yield a peak luminosity of

$$\mathcal{L} = \frac{3}{16\pi r_e^2 (m_e c^2)} \frac{P_{\text{SR}} \xi_y \rho}{\beta_y^* \gamma^3}, \quad (\text{III.4.5})$$

which scales approximately as $1/E_b^{3.5}$ (see Fig. 3 of Ref. [39]). The decrease of luminosity with higher energy is evident on the right-hand side of Fig. III.4.2. Table III.4.2 compares the design parameters for CEPC and FCC-ee with those achieved at the operating DAΦNE collider and with the design parameters of SuperKEKB.

The short beam lifetime at the high target luminosity, due to radiative Bhabha scattering, requires FCC-ee and CEPC to be constructed with a full-energy injector ring installed in the same tunnel to “top up” the electron and positron currents in the collider rings operating at constant energy. At highest

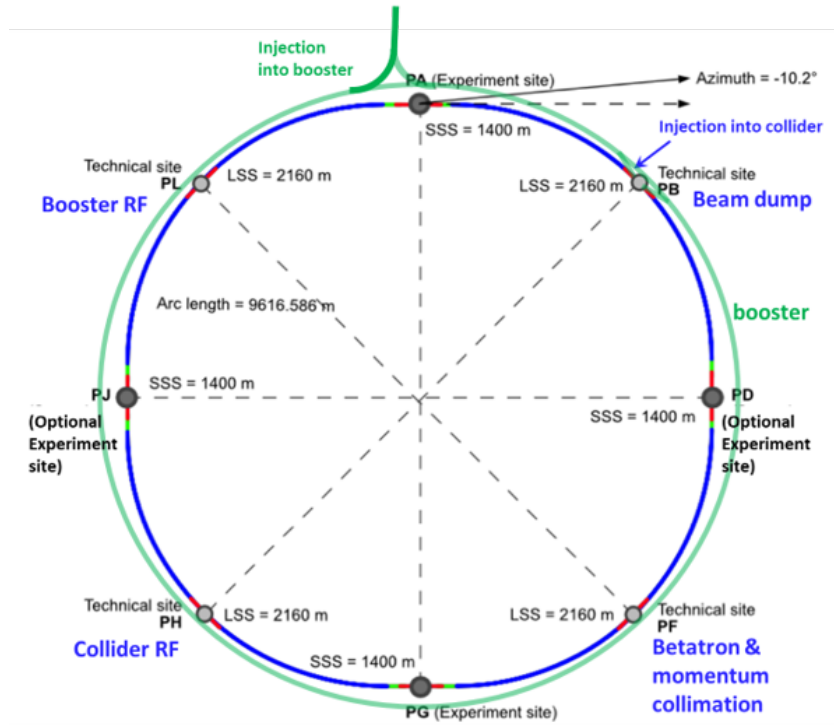


Fig. III.4.4: FCC-ee collider layout featuring a fourfold superperiodicity, with four interaction points, and four technical long straight sections. The full-energy booster is located in the same tunnel, but bypasses the experimental detectors. The distance between booster and collider is exaggerated and not to scale.

Table III.4.2: Key design parameters of FCC-ee and CEPC in Higgs production mode or on the Z pole compared with approximate values achieved at DAΦNE and with the SuperKEKB design [40].

collider	DAΦNE	SuperKEKB		FCC-ee Z	FCC-ee H	CEPC H (‘50 MW’)
		e ⁺	e ⁻			
beam energy E_b [GeV]	0.51	4	7	80	120	120
circumference C [km]	0.097	3.02		90.7	90.7	100
beam current I_b [A]	1.25	3.6	2.6	1.27	0.027	0.028
total SR power P_{SR} [MW]	0.02	12.7		100	100	100
bunch population N_b [10^{11}]	0.25	0.9	0.65	2.14	1.14	1.3
no. bunches / beam n_b	100	2500		11200	440	446
rms bunch length σ_z [mm]	15	6	5	15.5	4.7	4.1
horizontal IP beta β_x^* [m]	0.23	0.032	0.025	0.11	0.24	0.3
vertical IP beta β_y^* [mm]	8.5	0.27	0.3	0.7	1.0	1.0
Piwinski angle Φ	1.5	25	19	26	5.4	4.9
IP hor. rms beam size σ_x^* [μm]	250	10	11	9	13	14
IP vert. rms beam size σ_y^* [nm]	3100	48	62	36	40	36
luminosity/IP L [$10^{34} \text{ cm}^{-2}\text{s}^{-1}$]	0.05	80		140	5.0	8.3

energies (especially for $t\bar{t}$ operation), beamstrahlung introduces an additional beam lifetime limitation, which depends on the (relative) momentum acceptance δ_{\max} , [29, 30]

$$\frac{1}{\tau_{\text{bs}}} = \frac{1}{f_{\text{rev}} N_{\text{IP}}} \frac{4}{3 \cdot 2^{1/4}} \frac{1}{r_e^2 \alpha^{1/2}} \frac{\sigma_x^{*3/2} \sigma_z^{1/2} \delta_{\max}^{1/2} (1 + \Phi^2)^{1/2}}{\gamma^{1/2} N_b^{3/2}} \exp\left(\frac{\sqrt{2}}{3} \frac{\alpha}{r_e^2} \frac{\delta_{\max} \sigma_z \sigma_x^*}{\gamma N_b}\right), \quad (\text{III.4.6})$$

where α denotes the fine structure constant, N_{IP} the number of collision points, and $\Phi \equiv \theta_c \sigma_z / (2\sigma_x^*)$ the Piwinski angle. Most important is the argument of the exponential, which contains the factor $\sigma_z \sigma_x^* \delta_{\max} / \gamma$. In consequence, achieving a sufficient off-momentum dynamic aperture δ_{\max} becomes one of the design challenges. At lower energy, especially on the Z pole, multiple beamstrahlung photon emission causes significant increase in energy spread and associated bunch lengthening and, in case of nonzero dispersion at the collision point, also transverse emittance growth [31].

The ambitious, large-scale projects FCC-ee and CEPC could be (but need not be) realized using only well-established technologies. Though not extendable to TeV or multi-TeV energies, they offer several important advantages that include the potential for much higher luminosity, and, thus, higher precision, the ability to operate multiple experiments simultaneously, and their ~ 100 km circular tunnels that could later house $O(100 \text{ TeV})$ hadron colliders. The high energy efficiency inherent to circular e^+e^- colliders would be further boosted by advances in RF power sources, by improved SC cavities, and by innovative low-power magnet systems including ones based on high-temperature superconductors (HTS) at moderate magnetic field [41].

III.4.5.5 Beam polarisation and energy calibration

A few e^+e^- collider designs and proposals aim at colliding longitudinally polarised beams, with the help of spin rotators. More common is the use of transverse polarisation for a precise calibration of the average beam energy using resonant depolarisation, thanks to a simple relation linking the spin tune Q_s and the average beam energy E_b (for a storage ring with planar orbits): $E_b = 440.64843 \times Q_s$ [MeV]. Resonant depolarisation was successfully used to accurately measure the spin tune Q_s and, thereby, the beam energy, for example, at VEPP-2M [42], VEPP-4M [43] and LEP [44]. A precise calibration of the collision energy can be carried out in the Z and WW running modes of the proposed FCC-ee collider, using resonant depolarisation of pre-polarised pilot bunches. The FCC-ee design aims at achieving uncertainties of around 100 keV and 20 keV for the Z mass and width, respectively, to be compared to the equivalent numbers of 1.7 MeV and 1.2 MeV obtained at LEP.

III.4.5.6 Monochromatisation

For maximising the luminosity on a narrow resonance, monochromatisation can be used to reduce the collision energy spread so as to become smaller than the convoluted beam energy spread. Monochromatisation could be realised for example by introducing nonzero dispersion of opposite sign at the collision point, so that an electron with positive energy offset preferentially collides with positrons of negative momentum offset, and vice versa [46, 47]. For FCC-ee, colliding beams with an energy 62.5 GeV, at the peak of direct Higgs-production, $e^+e^- \rightarrow H$, is currently being studied, including monochromatisation, to measure the electron Yukawa coupling [39].

III.4.5.7 Outlook

More than 60 years after the first electrons and positrons collided in AdA, intense design efforts for future circular e^+e^- colliders are now being pushed forward. The actual and predicted performance of present and future e^+e^- colliders, respectively, continues to improve, thanks to the introduction of novel concepts, with the crab-waist collision scheme serving as a prime example, and thanks to the development of innovative technologies, with a great emphasis on sustainability. Several ambitious

circular e^+e^- collider projects are being pursued around the world. They are aimed at breaking new ground in both particle and accelerator physics, and at preparing a path for the long-term future of our fields.

References

- [1] C. Bernadini *et al.*, *Nuovo Cimento* **34**, 6 (1964) 1473–1493
- [2] A. Yu. Barnyakov and Super Charm-Tau Factory collaboration, *J. Phys.: Conf. Ser.* **1561**, 012004 (2020)
- [3] H. Ping, Y.H. Zheng, X. Rong, *Physics* **49**, 8 (2020) 513–524, [doi:10.7693/wl20200803](https://doi.org/10.7693/wl20200803)
- [4] V.D. Shiltsev and F. Zimmermann, *Rev. Mod. Phys.* **93**, 1, 015006 (2021)
- [5] M. Sands, *The Physics of Electron Storage Rings: An Introduction*, SLAC-121 (1969)
- [6] A.W. Chao, *AIP Conference Proceedings* **127**, 1 (1985) 201
- [7] N.S. Dikanskij and D.v Pestrikov, *Part. Acc.* **12** (1982) 27-37
- [8] A.W. Chao and R.D. Ruth, *Part. Acc.* **16** (1984) 201-216
- [9] K. Yokoya *et al.*, *Part. Accel.* **27** (1989) 181-186
- [10] Y.I. Alexahin, *Part. Accel.* **59** (1998) 43–74
- [11] S. Krishnagopal and R.H. Siemann, *Phys. Rev. Lett.* **67**, 18 (1991) 2461
- [12] A.V. Otbojev and E.A. Perevedentsev, *Phys. Rev. ST Accel. Beams* **2**, 10, 104401 (1999)
- [13] K. Ohmi, N. Kuroo, K. Oide, D. Zhou, and F. Zimmermann, *Phys. Rev. Lett.* **119**, 134801 (2017)
- [14] V. Shiltsev *et al.*, *Phys. Rev. Accel. Beams* **8**, 10, 101001 (2005)
- [15] J.T. Seeman, *Observations of the beam-beam interaction*, Springer Lecture Notes in Physics (1986) 121–153
- [16] R.W. Assmann, K. Cornelis, *The Beam-Beam Interaction in the Presence of Strong Radiation Damping*, Proc. **EPAC2000**, Vienna (2000) pp. 1187
- [17] V.D. Shiltsev, *Electron Lenses for Super-Colliders*, Springer (2016)
- [18] V.V. Danilov *et al.*, *The concept of round colliding beams*, Proc. **EPAC96**, Sitges (1996) 1149
- [19] E. Young *et al.*, *Collisions of Resonantly Coupled Round Beams at the Cornell Electron-Positron Storage Ring (CESR)*, Proc. **PAC97**, Vancouver (1998) 1542
- [20] D. Berkaev *et al.*, *Nuclear Physics B-Proceedings Supplements* **225** (2012) 303–308
- [21] Yu. Shatunov *et al.*, *Project of a new electron-positron collider VEPP-2000*, Proc. **EPAC 2000**, Vienna, Austria (2000) 439–441
- [22] K. Oide, K. Yokoya, *Phys. Rev. A* **40** (1989) 315-316, [doi:10.1103/PhysRevA.40.315](https://doi.org/10.1103/PhysRevA.40.315)
- [23] Y. Funakoshi, *Operational experience with crab cavities at KEKB*, Proc. ICFA Mini-Workshop on Beam-Beam Effects in Hadron Colliders (BB2013), CERN, Geneva, Switzerland, March 18-22 2013 (2014) 27–36, [doi:10.5170/CERN-2014-004.27](https://doi.org/10.5170/CERN-2014-004.27)
- [24] P. Raimondi, D. Shatilov, M. Zobov, *Beam-beam issues for colliding schemes with large Piwinski angle and crabbed waist*, [arXiv:physics/0702033](https://arxiv.org/abs/physics/0702033) (2007)
- [25] M. Zobov *et al.*, *Phys. Rev. Lett.* **104**, 17, 174801 (2010)
- [26] K. Ohmi, *Simulated Beam-beam Limits for Circular Lepton and Hadron Colliders*, Proc. **IPAC16**, Busan (2016)
- [27] M.A. Furman, Proc. **EPAC94**, London, England, June 27-July 1, 1994 (1994) 1144–1146
- [28] K. Hirata and F. Ruggiero, *Part. Accel.* **28** (1990) 137-142
- [29] V.I. Telnov, *Phys. Rev. Lett.* **110**, 114801 (2013)
- [30] A. Bogomyagkov, E. Levichev, D. Shatilov, *Phys. Rev. ST Accel. Beams* **17** (2014) 041004
- [31] M.A. Valdivia Garcia and F. Zimmermann, *Eur. Phys. J. Plus* **136**, 501 (2021)

-
- [32] D. Shatilov, *Eur. Phys. J. Plus* **137**, 159 (2022), [doi:10.1140/epjp/s13360-022-02346-x](https://doi.org/10.1140/epjp/s13360-022-02346-x)
- [33] Y. Funakoshi *et al.*, The SuperKEKB Has Broken the World Record of the Luminosity Proc. **IPAC22** (2022) 1–5
- [34] M. Yamauchi, KEK’s Physics Program in the Next 10 Years, U.S. P5 Meeting, BNL, 13 April 2023
- [35] K. Oide *et al.*, *Phys. Rev. Accel. beams* **19**, 111005 (2016)
- [36] A. Blondel, F. Zimmermann, A High Luminosity e+e- Collider in the LHC tunnel to study the Higgs Boson, [arXiv:1112.2518](https://arxiv.org/abs/1112.2518) (2011)
- [37] A. Abada *et al.*, *Eur. Phys. J. ST* **228**, 2 (2019) 261
- [38] CEPC Study Group, CEPC Conceptual Design Report: Volume 1 - Accelerator, [arXiv:1809.00285](https://arxiv.org/abs/1809.00285) (2018)
- [39] A. Faus-Golfe, M.A. Valdivia Garcia, F. Zimmermann, *Eur. Phys. J. Plus* **137** (2022) 31
- [40] K. Akai, K. Furukawa, H. Koiso, *Nucl. Instrum. Meth. A* **907** (2018) 188-199
- [41] V. Batsari, B. Auchmann, J. Kosse, M. Koratzinos, HTS4 project explores superconducting options for the FCC-ee, *Accelerating News* **44** (2023), acceleratingnews.eu
- [42] Ya.S. Derbenev *et al.*, *Part. Accel.* **8** (1978) 115-126
- [43] V.E. Blinov *et al.*, *Nucl. Part. Phys. Proc.* **273-275** (2016) 210-218
- [44] L. Arnaudon *et al.*, The energy calibration of LEP in 1991, CERN-SL-92-37-DI (1991) [cds:239962](https://cds.cern.ch/record/239962) (1991)
- [45] A. Blondel *et al.*, Polarization and Centre-of-mass Energy Calibration at FCC-ee, [arXiv:1909.12245](https://arxiv.org/abs/1909.12245) (2019)
- [46] A. Renieri, Possibility of Achieving Very High-Energy Resolution in electron-Positron Storage Rings, LNF-75/6-R (1975)
- [47] A. Faus-Golfe and J. Le Duff, *Nucl. Instrum. Meth. A* **372** (1996) 6–18